



# Calorimetric measurements of sodium chloride dihydrate (hydrohalite)

V. A. Drebuschak<sup>1,2</sup> · A. G. Ogienko<sup>2</sup>

Received: 22 March 2019 / Accepted: 25 October 2019 / Published online: 4 November 2019  
© Akadémiai Kiadó, Budapest, Hungary 2019

## Abstract

Calorimetric measurements of sodium chloride dihydrate  $\text{NaCl}\cdot 2\text{H}_2\text{O}$  (mineral name hydrohalite) were carried out with using DSC. Heat capacity from 190 to 250 K was measured and found to increase from 109 to 137  $\text{J mol}^{-1} \text{K}^{-1}$ . The enthalpy of formation of hydrohalite from solid ice and halite at 273.15 K was derived from the thermal effect of melting/decomposition in DSC measurements and found to be close to  $-1.8 \text{ kJ mol}^{-1}$ . The same DSC results show clearly that the upper temperature limit for the existence of hydrohalite is several degrees greater than the current value of 273.15 K accepted for the peritectic decomposition of hydrohalite. The phase diagram of the  $\text{NaCl}\text{--}\text{H}_2\text{O}$  system needs correction.

**Keywords** DSC · Enthalpy of formation · Heat capacity · Hydrohalite

## Introduction

Sodium chloride dihydrate  $\text{NaCl}\cdot 2\text{H}_2\text{O}$  (mineral name hydrohalite) occupies the central part of the  $\text{NaCl}\text{--}\text{H}_2\text{O}$  system and is used widely in modeling natural processes in very different fields of science: thermal budget of planets [1, 2] and their satellites [3], planet surface morphology and weathering [4–6], Earth fluid dynamics [7], metamorphism [8], and life on Mars [9]. The reliability of modeling depends on adequate relationships among variables involved in the evaluations and accuracy of input data for the calculations. Surprisingly, there were no direct calorimetric measurements of hydrohalite so far.

Thermodynamic properties of hydrohalite were derived from rather complex considerations (the enthalpy of formation) or estimated by analogy with other hydrates of salts (heat capacity and entropy) [10].

Direct calorimetric measurements of hydrohalite were impossible because of the problems with the crystallization of sufficient amount of samples. For many years, the works on experimental investigations of hydrohalite report about difficulties with its crystallization. Recently, the problem

was solved and the procedure of fast hydrohalite crystallization in sufficient amount (hundreds grams in one batch) was developed [11].

The objective of this study was to measure the heat capacity of hydrohalite and its enthalpy of melting/decomposition.

## Experimental

### Sample

The crystals of hydrohalite were grown from water solution of  $\text{NaCl}$  (purity 99.7%) after the decrease in temperature below 255 K. The solution was prepared at room temperature with a layer of unsolved salt at the bottom of the flasks and then exposed to low temperature ( $\sim 253 \text{ K}$ ). Several hours later, the layer of hydrohalite crystals ( $\sim 1 \text{ cm}$  in size) grown on the bottom (on the surface of a strong frozen layer of  $\text{NaCl} + \text{NaCl}\cdot 2\text{H}_2\text{O}$ ) was found. The solution was poured out and fragile hydrohalite crystals were scrapped from the strong substrate. The crystals are very wet, and excess liquid is absorbed partially with cotton fabric. Then, the crystals are packed in bottles and kept at 255 K. The whole procedure of hydrohalite crystallization is described in [11]. Harvesting the crystals is shown in movie ([https://www.youtube.com/watch?v=\\_V9sy20C5qI](https://www.youtube.com/watch?v=_V9sy20C5qI)). The soft layer of hydrohalite crystals and strong substrate are shown in another movie (<https://www.youtube.com/watch?v=1ekaPbyW7P0>).

✉ V. A. Drebuschak  
dva@igm.nsc.ru

<sup>1</sup> V.S. Sobolev Institute of Geology and Mineralogy, SB RAS,  
Pr. Ak. Koptyuga, 3, Novosibirsk, Russia 630090

<sup>2</sup> Novosibirsk State University, Pirogova, 2, Novosibirsk,  
Russia 630090

For calorimetric measurements, a portion of hydrohalite crystals (~ 10 g) was ground in a metal mortar kept in liquid nitrogen. The grinding was rather mild because it was necessary only to destroy large crystals (~ 1 cm) into small fragments to fill DSC crucibles of 5 mm in diameter and 3-mm tall.

The sample consists of solid hydrohalite crystals and remnant solution covering the surface of the crystals. To define the ratio of solid and liquid phases, we have filled a crucible of mass  $M_0$  with a sample and measured its mass ( $M_1$ ). Then, the sample in the crucible was stored under room conditions for a long time until its mass became constant. The crucible contained dry salt and its mass was  $M_2$ . The NaCl content in the sample was calculated after ratio  $(M_2 - M_0)/(M_1 - M_0)$  and found to be 0.5907. The salt content of stoichiometric hydrohalite (NaCl·2H<sub>2</sub>O) is 0.6186.

Below the temperature of equilibrium eutectic melting (251.9 K), our sample is a mixture of solid phases, hydrohalite and ice, with composition NaCl·2H<sub>2</sub>O + 0.248H<sub>2</sub>O. Above that temperature, the sample is a mixture of solid hydrohalite with its aqueous solution:  $x \{ \text{NaCl} \cdot y\text{H}_2\text{O} \} + (1 - x) \text{NaCl} \cdot 2\text{H}_2\text{O}$ . The curly brackets are for the composition of solution. The solubility of hydrohalite changes with temperature and the values of  $x$  and  $y$  change with temperature too. At the eutectic temperature, the salt content of the equilibrium aqueous solution is 0.2316 and our sample is 0.0283{NaCl·10.673H<sub>2</sub>O} + 0.9717NaCl·2H<sub>2</sub>O at 252 K. At the peritectic temperature, the salt content of equilibrium aqueous solution is 0.2627 and our sample is 0.0349{NaCl·9.105H<sub>2</sub>O} + 0.9651NaCl·2H<sub>2</sub>O at 273 K.

## DSC

Calorimetric experiments were carried out using DSC-204 Netzsch with TA Controller 414/3 and liquid nitrogen Combi-Cooler CC 200, in a flow of dry argon (30 mL min<sup>-1</sup>). Standard aluminum crucibles (25 μL) were covered with a lid, but not sealed in order to provide a free output of water vapor after the melting/decomposition of hydrohalite. Recommended temperature fixed points are reproduced with the accuracy of ±0.1 K. Two temperature programs were used. The first one was from 173 to 268 K (-100 to -5 °C) at a heating rate of 6 K min<sup>-1</sup>. The second one was from 230 to 383 K (-43 to +110 °C) at the heating rates of 3 K min<sup>-1</sup>. Before the measurements, the DSC cell was cooled down to 115 K (starting from 173 K; heating with 6 K min<sup>-1</sup>) or 190 K (starting from 230 K; heating with 3 K min<sup>-1</sup>) and kept isothermally for some time. Then, the cooling system was switched off, and the temperature of the DSC cell increases “naturally” up to room temperature, with the heating rate decreasing exponentially. Preliminary cooling was arranged in such a way that the natural heating rate was less than 6 K min<sup>-1</sup> above 173 K or 3 K min<sup>-1</sup> above

230 K. Thus, the measurements were carried out without the cooling system working. Such a procedure yields extremely low noise in the DSC signal as compared with conventional measurements when the cooling system works.

In fulfilling the demand by anonymous reviewer, we explain here that the heating rate of 6 K min<sup>-1</sup> was chosen for the measurements of heat capacity of hydrohalite because after examination of technical characteristics of our DSC-204 Netzsch about 15 years ago, this value was found to be close to optimal for the measurements of nonmetals (insulators) with low thermal conductivity. Some higher heating rate needs significantly lower starting temperature without any improvement in the accuracy. Some lower heating rate decreases signal-to-noise ratio and makes the temperature interval of the measurements some shorter. The heating rate of 3 K min<sup>-1</sup> for the decomposition of hydrohalite was chosen because 6 K min<sup>-1</sup> turned out to be too fast for the evaporation of water from the sample. The brine formed after the decomposition of hydrohalite was partly splashed out of the crucible at 6 K min<sup>-1</sup>, but not at 3 K min<sup>-1</sup>. Also, it is not interesting to perform the measurements of hydrohalite at both heating rates of 6 and 3 K min<sup>-1</sup> in order to compare them after because the results of this kind say nothing about the hydrohalite. They can characterize the DSC, but the characterization must be performed on the standard (recommended) samples, for example, copper (metal), corundum (nonmetal), and benzoic acid (organic). The measurements of this kind were performed with our DSC-204 Netzsch many years ago.

## Measurement programs

Empty crucible was weighed ( $m_0$ ) and then placed into the bath with liquid nitrogen, close to the metal mortar with prepared (crushed crystals of hydrohalite) sample. The crucible was filled with the sample, covered with a lid, and then placed onto the sample holder inside the DSC cell at 260 K. It was the starting point for a series of measurements with the same sample. All the results of the measurements were the raw data with the signal measured in μV, without the calibration of heat-flux sensor. The series will be referred below as  $U_i$  after the number of temperature program ( $i = 1, 2, 3, 4$ ).

The first series ( $U_1$ ) is after the measurements from 173 to 268 K at 6 K min<sup>-1</sup>. The regular signal is proportional to the heat capacity of starting sample (hydrohalite + ice below 252 K and hydrohalite + solution above), with anomalous signal from the eutectic melting at 252 K. After the completion of that series, the sample was cooled down to 190 K and transformed back to the solid mixture of hydrohalite and ice.

The second series ( $U_2$ ) is after the measurements from 230 to 383 K at 3 K min<sup>-1</sup>. Regular signal is proportional to the heat capacity of starting sample (hydrohalite + ice below

252 K, hydrohalite + solution between 252 K and melting/decomposition of hydrohalite, aqueous solution of NaCl (above), with anomalous signal because of eutectic melting (starting from 252 K), melting/decomposition of hydrohalite, and evaporation of aqueous solution of NaCl. After the completion of that series, the sample was cooled down to 115 K and consisted of dry salt.

The third series ( $U_3$ ) is after the measurements from 173 to 268 K at 6 K min<sup>-1</sup>. The regular signal is proportional to the heat capacity of NaCl. After the completion of that series, the sample was cooled down to 190 K.

The fourth ( $U_4$ ) is after the measurements from 230 to 383 K at 3 K min<sup>-1</sup>. The regular signal is proportional to the heat capacity of NaCl. It was the last measurement in the series. After the completion, the sample was taken off the DSC and weighed ( $m_2$ ) for measuring the salt mass ( $m_2 - m_0$ ).

Totally, four series of the measurements were carried out with four samples (with salt mass of 10.87, 9.88, 13.84, and 12.87 mg). These provide us with four data sets ( $j$ ) for every temperature program ( $i$ ):  $U_{1j}$ ,  $U_{2j}$ ,  $U_{3j}$ ,  $U_{4j}$  ( $j=1, 2, 3, 4$ ).

The measurements of the empty crucible (blank run) were carried out only for series  $U_1$  and will be referred below as  $U_0$ . The crucible was placed onto the sample holder inside DSC at temperature 260 K, and the measurement was carried out from 173 to 268 K at 6 K min<sup>-1</sup>. After the completion of the run, the crucible was taken out of the DSC. Then, the DSC with only reference crucible and without sample crucible was heated up to 323 K and cooled down to 260 K again for the next blank run. This procedure allows us to diminish the positioning bias [12]. Totally, five blank runs were carried out.

## Heat capacity evaluations

The conventional procedure of the heat capacity measurements with DSC under scanning heating is based on the formula

$$c_s(T) = k(T) \frac{1}{m_s} \frac{1}{\beta} (U_s(T) - U_0(T)), \quad (1)$$

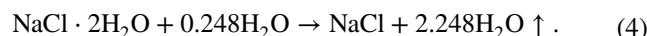
where  $m_s$  is the sample mass,  $k(T)$  is the calibration coefficient,  $\beta$  is the heating rate,  $U_s$  is the DSC signal measured for the crucible with a sample, and  $U_0$  is the DSC signal from empty crucible (blank run). Strictly speaking,  $c_s(T)$  should be named “specific heat,” not “heat capacity,” because it ( $c_s$ ) is normalized per mass unit as opposed to that ( $C_s$ ) normalized per mole. In fulfilling the demand by anonymous reviewer, we state here that no limitations for  $\beta$  values in Eq. (1) were ever published and it means that the equation is valid for any beta. When measuring a sample with known specific heat (reference substance), we have

$$c_r(T) = k(T) \frac{1}{m_r} \frac{1}{\beta} (U_r(T) - U_0(T)). \quad (2)$$

Dividing Eq. (1) by Eq. (2), we have

$$\frac{c_s(T)}{c_r(T)} = \frac{m_r}{m_s} \frac{(U_s(T) - U_0(T))}{(U_r(T) - U_0(T))}. \quad (3)$$

In our experiments,  $c_s(T)$  is the specific heat of starting sample NaCl·2H<sub>2</sub>O + 0.248H<sub>2</sub>O and  $U_s = U_1$ , while  $c_r(T)$  is the specific heat of dry NaCl after the decomposition of hydrohalite and evaporation of water and  $U_r = U_3$ . The values of  $U_0(T)$ ,  $U_1(T)$ ,  $U_3(T)$ , and  $m_r$  were measured, and  $c_r(T)$  is the reference data. To calculate  $c_r(T)$ , we need only  $m_s$ . It can be derived from the equation of the chemical reaction



If denoting formula weight of starting sample (left-hand side of Eq. 4)  $\mu_s$  and formula weight of dry salt  $\mu_r = \mu_{\text{NaCl}}$ , we have

$$m_s = m_r \frac{\mu_s}{\mu_r}. \quad (5)$$

In our experiments, the reference substance is NaCl and its specific heat  $c_r(T) = c_{\text{NaCl}}(T)$ . Using Eq. (5), Eq. (3) transforms finally into

$$\frac{\mu_s c_s(T)}{\mu_{\text{NaCl}} c_{\text{NaCl}}(T)} = \frac{(U_{1j}(T) - \overline{U_0}(T))}{(U_{3j}(T) - \overline{U_0}(T))}, \quad (6)$$

where  $U_{1j}(T)$  and  $U_{3j}(T)$  are the results of the measurements for particular sample  $j$  and  $\overline{U_0}(T)$  is the average baseline after five blank runs. Surprisingly, the sample mass is absent from the formula for the calculation of the specific heat of our starting sample after the specific heat of dry salt obtained after the decomposition of the sample. It is because the sample mass and dry salt mass are related to strict proportion: the greater the sample mass, the greater the mass of dry salt, and their ratio is constant. Our experimental procedure provides us with one more benefit. As the measurements of investigated substance (starting sample) and those of reference (dry salt) are carried out after the single placing of the crucible at the sample holder, the positioning bias is excluded. The accuracy of our calculations of the sample heat capacity becomes better.

Equation (6) allows us to derive the heat capacity of the starting sample after DSC measurements. But, the starting sample is not pure hydrohalite. It is a mixture of hydrohalite with ice. Let us remember that the product of specific heat ( $c_p$ ) by the formula weight ( $\mu$ ) is the molar heat capacity:  $C_p = \mu \cdot c_p$ . For temperatures below eutectic melting, molar heat capacity of the sample is the sum of molar heat capacity of hydrohalite ( $C_{\text{hh}}$ ) and portion of

heat capacity of ice ( $C_{ice}$ ). For our reference substance (dry salt), the product is the molar heat capacity of NaCl:  $C_{NaCl} = \mu_{NaCl} \cdot c_{NaCl}$ . Finally, we have

$$C_{hh}(T) + 0.248C_{ice}(T) = C_{NaCl}(T) \frac{(U_{1j}(T) - \bar{U}_0(T))}{(U_{3j}(T) - \bar{U}_0(T))}. \quad (7)$$

All experimental results for every sample ( $j$ ) are combined into the fraction on the right-hand side of Eq. (7). For convenience, we will denote it

$$R_j(T) = \frac{(U_{1j}(T) - \bar{U}_0(T))}{(U_{3j}(T) - \bar{U}_0(T))}. \quad (8)$$

## Results and discussion

### Thermal effects in the sample

The DSC results used for the evaluation of the heat capacity of hydrohalite after Eq. (7) are shown in Fig. 1 for sample N4. The results for other samples show very similar figures. The bottom line is the average baseline ( $\bar{U}_0(T)$ , empty crucibles), the upper line is for the crucible with starting sample ( $U_{14}$ ), and the middle line is for the crucible with dry salt ( $U_{34}$ ). Before the start of a run, temperature inside DSC cell increases “naturally” with the heating rate of about 2–3 K min<sup>-1</sup>. Immediately after the start of the run with heating rate of 6 K min<sup>-1</sup>, the step response takes place in the DSC signal. The signal stabilizes near 190 K, and this is the low temperature limit for the data that can be used for the evaluation of the heat capacity. The eutectic melting starts near 252 K. Its heat effect is seen in Fig. 1 as the endothermic peak on line  $U_1$ .

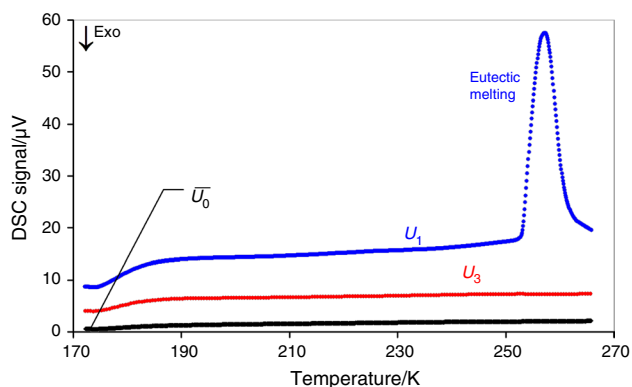


**Fig. 1** DSC results for sample N4 at a heating rate of 6 K min<sup>-1</sup> used for the calculations of heat capacity after Eq. (7):  $U_1$ —starting sample,  $U_3$ —dry NaCl after the decomposition of hydrohalite and the evaporation of resulting aqueous solution,  $\bar{U}_0$ —empty crucible

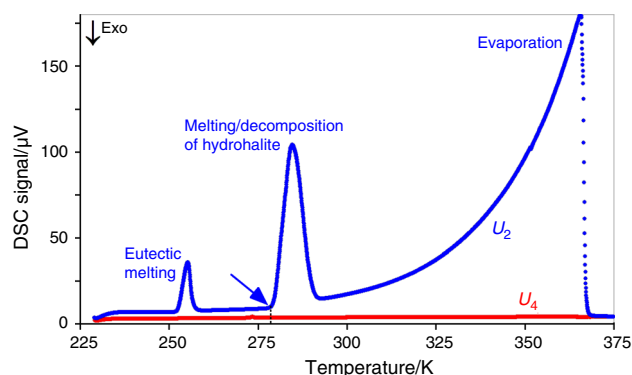


**Fig. 2** DSC results for sample N1 at a heating rate of 3 K min<sup>-1</sup>:  $U_2$ —starting sample,  $U_4$ —dry NaCl after the decomposition of hydrohalite and the evaporation of resulting aqueous solution

The DSC results at a heating rate of 3 K min<sup>-1</sup> are shown in Fig. 2 for sample N1. Again, the results for other samples show very similar figures. Three endothermic effects are well seen in line  $U_2$ : (1) eutectic melting starting from 252 K, (2) melting/decomposition of hydrohalite above 275 K, and (3) evaporation of the aqueous solution. The evaporation finishes near 370 K and the sample becomes a dry salt. The DSC results for the dry salt are shown as line  $U_4$ .

### Heat capacity of hydrohalite

The heat capacity of hydrohalite was calculated after Eq. (7). Input data are listed in Table 1. All experimental values of  $U_{1j}(T)$  and  $U_{3j}(T)$  were smoothed for all temperatures except 250 K. The smoothing was made with using Netzsch Proteus software with window width “6,” data acquisition rate 60 points min<sup>-1</sup>. For 250 K, the peak of eutectic melting affects (corrupts) the smoothed values, and the smoothing was made “by hand.” The endothermic eutectic melting makes it impossible to measure the heat capacity of hydrohalite above 252 K for our experimental conditions.

All experimental data were used to calculate values  $R_j$  listed in Table 1 for each temperature and each sample. Average values  $\bar{R}$  with their standard deviations (in round brackets) for all temperatures are listed in Table 2. Heat capacities of NaCl were taken from [13], smoothing ours. Heat capacities of hexagonal ice Ih were taken from [14]. Final heat capacities of hydrohalite were calculated after the equation

$$C_{hh}(T) = \bar{R}(T)C_{NaCl}(T) - 0.248C_{ice}(T). \quad (9)$$

The heat capacity of hydrohalite was never measured before, and we can only compare our experimental values with those estimated. Donald G. Archer (1992) has calculated the heat capacity of hydrohalite at 298.15 K as a sum of the heat capacity of NaCl with “an approximate

**Table 1** Input data (DSC signal in  $\mu\text{V}$ ) for the calculation of hydrohalite heat capacity

T/K	$\overline{U_0}$	N1			N2			N3			N4		
		$U_{11}$	$U_{31}$	$R_1$	$U_{12}$	$U_{32}$	$R_2$	$U_{13}$	$U_{33}$	$R_3$	$U_{14}$	$U_{34}$	$R_4$
190	1.185	10.119	4.689	2.550	9.501	4.495	2.513	13.274	5.921	2.553	13.849	6.289	2.481
200	1.356	10.547	4.884	2.605	9.914	4.629	2.615	13.856	6.208	2.576	14.248	6.434	2.539
210	1.474	10.928	5.045	2.647	10.302	4.798	2.656	14.231	6.375	2.603	14.571	6.555	2.578
220	1.590	11.461	5.252	2.695	10.822	5.021	2.691	14.783	6.533	2.669	15.094	6.705	2.640
230	1.713	11.971	5.452	2.743	11.354	5.200	2.765	15.431	6.674	2.765	15.575	6.852	2.697
240	1.824	12.729	5.642	2.856	11.996	5.313	2.915	16.122	6.882	2.827	16.147	7.046	2.743
250	1.893	13.803	5.870	2.995	12.851	5.430	3.098	16.606	7.024	2.867	17.258	7.165	2.914

Column “ $R_j$ ” was calculated after Eq. (8)

**Table 2** Heat capacity of hydrohalite calculated after Eq. (9)

T/K	$\overline{R}$	$C_p/\text{J mol}^{-1} \text{K}^{-1}$		
		NaCl Ref. [13]	H <sub>2</sub> O ice Ih Ref. [14]	NaCl·2H <sub>2</sub> O This work
190	2.524 (0.034)	46.12	26.9973	109.7 (1.6)
200	2.584 (0.034)	46.68	28.2546	113.6 (1.6)
210	2.621 (0.037)	47.20	29.5249	116.4 (1.7)
220	2.674 (0.025)	47.68	30.8068	119.9 (1.2)
230	2.743 (0.032)	48.12	32.0998	124.1 (1.5)
240	2.835 (0.072)	48.52	33.4020	129.3 (3.5)
250	2.969 (0.101)	48.88	34.7127	136.5 (4.9)

value for the heat capacity contribution for two waters of hydration”:  $137 \text{ J mol}^{-1} \text{K}^{-1}$  [10]. That contribution of  $87 \text{ J mol}^{-1} \text{K}^{-1}$  was, in turn, compared with the contribution of  $83 \text{ J mol}^{-1} \text{K}^{-1}$  used in the previous work by Pabalan and Pitzer (1987) on the heat capacity of hydrates [15]. Recently, a new estimate of the heat capacity of hydrohalite was published by Schlaikjer et al. (2017):  $230.1 \text{ J mol}^{-1} \text{K}^{-1}$  at 298.15 K [16]. That value is surely incorrect, most likely because of misprint. The calculations were similar to those by Archer (1992) and Pabalan and Pitzer (1987), but with the “hydration contribution” of  $80 \text{ J mol}^{-1} \text{K}^{-1}$ . Anyway, all the estimations were made for 298.15 K, where hydrohalite does not exist.

**Melting/decomposition of hydrohalite**

The heat effect of the melting/decomposition of hydrohalite was calculated as the peak area seen in line  $U_2(T)$  in Fig. 2.

**Table 3** Evaluation of the enthalpy of melting/decomposition of hydrohalite

N	$\Delta Q/\text{mJ}$	$m_{\text{NaCl}}/\text{mg}$	$m_{\text{hh not corr.}}/\text{mmol}$	$m_{\text{hh corr.}}/\text{mmol}$	$\Delta_{\text{tr}}H/\text{J mol}^{-1}$
1	2501	10.87	0.1860	0.1795	13,933
2	2257	9.88	0.1691	0.1631	13,832
3	3243	13.84	0.2368	0.2285	14,192
4	2984	12.87	0.2202	0.2125	14,040
Avg.					13,999 (154)

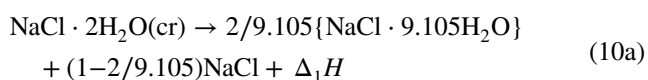
The calibration coefficient was calculated as the mean value of  $k(T)$  calculated after Eq. (2) using the experimental results for four series of dry NaCl measurements.

Input data and the results of the calculations are shown in Table 3. The heat effect of the melting/decomposition of hydrohalite is shown in column “ $\Delta Q$ .” The next column is for the dry NaCl mass after the decomposition of the sample and evaporation of aqueous solution formed. That mass in milligrams was recalculated into millimoles of NaCl. Below the eutectic temperature, the sample consists only of ice and hydrohalite, and the amount of NaCl·2H<sub>2</sub>O in millimoles is equal to the amount of dry NaCl in millimoles. The maximum amount of hydrohalite in a sample is shown in column “ $m_{\text{hh not corr.}}$ ” Above the eutectic temperature, hydrohalite is partially dissolved in aqueous solution, and the amount of crystalline hydrohalite decreases. The higher the temperature of the solution, the less the amount of solid hydrohalite in the sample. According to the phase diagram, the quantity of solid hydrohalite in a sample is the least at the peritectic temperature. That amount is shown in column “ $m_{\text{hh corr.}}$ ” The enthalpy of melting/decomposition of hydrohalite is shown in the last column “ $\Delta_{\text{tr}}H$ .” It was derived from the heat effect  $\Delta Q$  divided by amount “ $m_{\text{hh corr.}}$ ” The mean value after four experiments is  $13,999 \text{ J mol}^{-1}$  with the standard deviation of  $154 \text{ J mol}^{-1}$ .

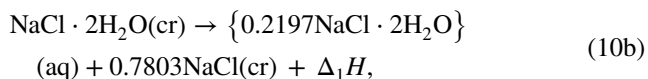
The enthalpy of melting/decomposition of hydrohalite allows us to estimate its enthalpy of formation from pure solid phases, ice and halite. The decomposition of hydrohalite produces a portion of solid NaCl and aqueous solution of NaCl. The composition of the aqueous solution at 273.15 K



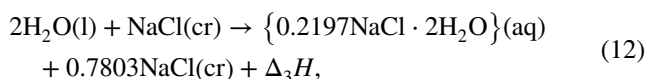
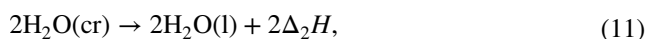
is  $\text{NaCl} \cdot 9.105\text{H}_2\text{O}$ . The thermochemical equation for that reaction is



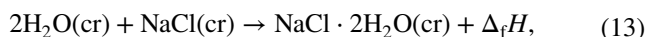
or



where  $\Delta_1 H$  is the enthalpy of melting/decomposition reported in Table 3. The same composition can be produced after the melting of 2 mol of ice and partial dissolution of 1 mol of halite in liquid water:



where  $\Delta_2 H$  is the enthalpy of ice melting and  $\Delta_3 H$  is the enthalpy of NaCl dissolution in water to saturation. Both variants, reaction (10) and melting (11) + dissolution (12), result in the same product (solid halite in its aqueous solution), but start from different initial reagents. To finish the thermochemical cycle, one should add the formation of hydrohalite from solid ice and halite:



where  $\Delta_f H$  is the enthalpy of formation of hydrohalite from ice and halite. The sum of heat effects in (10) + (13) is equal to the sum of heat effects in (11) + (12). This allows us to calculate the enthalpy of formation of hydrohalite from ice and halite:

$$\Delta_f H = -\Delta_1 H + 2\Delta_2 H + \Delta_3 H. \quad (14)$$

The enthalpy of ice melting is  $6007 \text{ J mol}^{-1}$  [14]. The enthalpy of NaCl dissolution in the water near 273.15 K for the molality ranging from 0.091 to 6.080 was published in [17]. According to [18], the molality of saturated aqueous solution of NaCl at 273.15 K is 6.097. The total enthalpy of NaCl dissolution in 1000 g of water up to its saturation is 6.19 kJ. The same enthalpy for two moles of water is 223 J. Thus, we have

$$\Delta_f H = -\Delta_1 H + 2\Delta_2 H + \Delta_3 H = -13,999 + 12,014 + 223 = -1762 \text{ J mol}^{-1}. \quad (15)$$

While estimating the accuracy of the resulting value, we can discuss only our own experimental data, with two contributions in the errors. First, it is the standard deviation of the peak area for  $\Delta_1 H$  ( $154 \text{ J mol}^{-1}$ ). Second, it is a possible error in the calibration coefficient of 1.5% or  $210 \text{ J mol}^{-1}$ .

Finally, we estimate the enthalpy of hydrohalite formation from ice and halite as  $-1762(364) \text{ J mol}^{-1}$ . This value was estimated for the peritectic reaction at 273.15 K, but our results show clearly that this assumption is wrong.

It is interesting to compare our melting/decomposition of hydrohalite with the peritectic reaction for sodium borohydride dihydrate ( $\text{NaBH}_4 \cdot 2\text{H}_2\text{O}$ ). The phase diagram of  $\text{NaBH}_4\text{-H}_2\text{O}$  system is very similar to that of  $\text{NaCl-H}_2\text{O}$  system, with identical topology, but different values of eutectic and peritectic temperatures and compositions [19]. Measured enthalpy of the peritectic reaction for  $\text{NaBH}_4 \cdot 2\text{H}_2\text{O}$  starting near 310 K was found to be  $19 \pm 2 \text{ kJ mol}^{-1}$  [20], rather close to our  $14 \text{ kJ mol}^{-1}$  near 280 K for  $\text{NaCl} \cdot 2\text{H}_2\text{O}$ .

Phase change materials (PCM) are the hot topic in renewable and sustainable energy management [21]. The most important characteristics of these materials are their heat of fusion and melting point. Sodium chloride dihydrate ( $148 \text{ J g}^{-1}$  at  $\sim 280 \text{ K}$ ) looks rather competitive as compared with the conventional PCMs, for example, organic substance  $\text{C}_{10}\text{H}_{10}\text{O}_2$  ((E)-3-phenylbut-2-enoic acid with  $130 \text{ J g}^{-1}$  at  $\sim 368 \text{ K}$ ) [22] and inorganic aqueous solution of  $\text{CaCl}_2 + \text{Ca}(\text{NO}_3)_2 + \text{SrCl}_2$  (with  $155.5 \text{ J g}^{-1}$  at  $\sim 275 \text{ K}$ ) [23]. It surely looks preferable as compared with the PCM for food storage, aqueous solution of mixture  $\text{Na}_2\text{SO}_4 \cdot 10\text{H}_2\text{O} + \text{Na}_2[\text{B}_4\text{O}_5(\text{OH})_4] \cdot 8\text{H}_2\text{O} + (\text{C}_3\text{H}_3\text{NaO}_2)_n + \text{NH}_4\text{Cl} + \text{KCl}$  (with  $141 \text{ J g}^{-1}$  at  $\sim 280 \text{ K}$ ) [24].

### The temperature of melting/decomposition of hydrohalite

From the very beginning, this work was based on the conventional phase diagram of the  $\text{NaCl-H}_2\text{O}$  system, where hydrohalite is thought to exist below the peritectic temperature at 273.15 K [18]. The heat capacity measurements were planned not to heat the sample above that temperature point. Now, after the completion of the DSC measurements of hydrohalite, we are sure that the upper temperature limit for hydrohalite to exist is not exactly at 273.15 K, but several degrees higher. The onset point of the melting/decomposition peak reported in this work is about 6.5 K higher. It is seen very well in Fig. 2 (arrow).

Surprisingly, this finding agrees with the information about the properties of hydrohalite published 225 years ago. It was reported in the very first paper about the existence of sodium chloride dihydrate that the crystals melt at  $143^\circ\text{D}$  (the Delisle scale) =  $277.8 \text{ K}$  [25, 26]. Our own measurements on separate crystals (not reported in this work) revealed that the onset point of the melting/decomposition peak can exceed the canonic value of 273.15 K by as high as 8 K. Perhaps, the upper temperature limit of existence for hydrohalite is governed not by peritectic reaction, but by liquidus line.

Having problem with the correct temperature and nature of melting/decomposition of hydrohalite, we think it is reasonable to clarify this question before the improvement in the accuracy of the enthalpy measurements. This is the problem for the next works.

## Conclusions

We have measured the heat capacity and thermal effects of melting/decomposition for hydrohalite for the first time ever. The experimental values of the heat capacity are known now as a function of temperature from 190 to 250 K. All previous theoretical estimations were made for the single temperature point of 298.15 K, where crystalline hydrohalite does not exist. The thermal effect of transformation (melting/decomposition) of solid hydrohalite into solid halite in its aqueous solution results in the estimate of  $-1762(364)$  J mol<sup>-1</sup> for the enthalpy of formation of hydrohalite from solid ice and halite. This estimate was made for conventional upper temperature limit of hydrohalite existence at 273.15 K. But, our experimental results show clearly that the true upper temperature limit is some degrees above that conventional value. The phase diagram of the NaCl–H<sub>2</sub>O system needs correction at this point.

**Acknowledgements** VAD acknowledges that his work was supported by state assignment Project No. 0330-2019-0004.

## References

- Carns RC, Light B, Warren SG. The spectral albedo of sea ice and salt crusts on the tropical ocean of Snowball Earth: II. Optical modeling. *J Geophys Res Oceans*. 2016;121:5217–30. <https://doi.org/10.1002/2016JC011804>.
- Shields AL, Carns RC. Hydrohalite salt-albedo feedback could cool M-dwarf planets. *Astrophys J*. 2018;867:11. <https://doi.org/10.3847/1538-4357/aadcaa>.
- Valenti P, Bodnar RJ, Schmidt C. Experimental determination of H<sub>2</sub>O–NaCl liquids to 25 mass% NaCl and 1.4 GPa: application to the Jovian satellite Europa. *Geochim Cosmochim Acta*. 2012;92:117–28. <https://doi.org/10.1016/j.gca.2012.06.007>.
- Flahaut J, Martinot M, Bishop JL, Davies GR, Potts NJ. Remote sensing and in situ mineralogical survey of the Chilean salars: an analog to Mars evaporate deposits? *Icarus*. 2017;282:152–73. <https://doi.org/10.1016/j.icarus.2016.09.041>.
- Ward MK, Pollard WH. A hydrohalite spring deposit in the Canadian high Arctic: a potential Mars analogue. *Earth Planet Sci Lett*. 2018;504:126–38. <https://doi.org/10.1016/j.epsl.2018.10.001>.
- Fateev EG. Anomalously low elastic stability of NaCl–H<sub>2</sub>O ice at low temperatures. *Tech Phys*. 2010;55:958–64. <https://doi.org/10.1134/S1063784210070078>.
- Butler BM, Papadimitriou S, Day SJ, Kennedy H. Gypsum and hydrohalite dynamics in sea ice brines. *Geochim Cosmochim Acta*. 2017;213:17–34. <https://doi.org/10.1016/j.gca.2017.06.020>.
- Steele-MacInnis M, Bodnar RJ. Effect of the vapor phase on the salinity of halite-bearing aqueous fluid inclusions estimated from the halite dissolution temperature. *Geochim Cosmochim Acta*. 2013;115:205–16. <https://doi.org/10.1016/j.gca.2013.04.009>.
- Davila AF, Duport LG, Melchiorri R, Jänchen J, Valea S, de los Rios A, Fairén AG, Möhlmann D, McKay CP, Ascaso C, Wierzchos J. Hygroscopic salts and the potential for life on Mars. *Astrobiology*. 2010;10:617–28. <https://doi.org/10.1089/ast.2009.0421>.
- Archer DG. Thermodynamic properties of the NaCl + H<sub>2</sub>O system. II. Thermodynamic properties of NaCl (aq), NaCl·2H<sub>2</sub>O (cr), and phase equilibria. *J Phys Chem Ref Data*. 1992;21:793–829. <https://doi.org/10.1063/1.555915>.
- Drebushchak VA, Drebushchak TN, Ogienko AG, Yunoshev AS. Crystallization of sodium chloride dihydrate (hydrohalite). *J Cryst Growth*. 2019;517:17–23. <https://doi.org/10.1016/j.jcrysgro.2019.04.009>.
- Pishchur DP, Drebushchak VA. Recommendations on DSC calibration: how to escape the transformation of a random error into the systematic error. *J Therm Anal Calorim*. 2016;124:951–8. <https://doi.org/10.1007/s10973-015-5186-8>.
- Archer DG. Enthalpy increment measurements for NaCl (cr) and KBr (cr) from 4.5 K to 350 K, thermodynamic properties of the NaCl + H<sub>2</sub>O system. 3. *J Chem Eng Data*. 1997;42:281–92. <https://doi.org/10.1021/jc960224q>.
- Feistel R, Wagner W. A new equation of state for H<sub>2</sub>O ice Ih. *J Phys Chem Ref Data*. 2006;35:1021–47. <https://doi.org/10.1063/1.2183324>.
- Pabalan RT, Pitzer KS. Thermodynamics of concentrated electrolyte mixtures and the prediction of mineral solubilities to high temperatures for mixtures in the system Na–K–Mg–Cl–SO<sub>4</sub>–OH–H<sub>2</sub>O. *Geochim Cosmochim Acta*. 1987;51:2429–43. [https://doi.org/10.1016/0016-7037\(87\)90295-X](https://doi.org/10.1016/0016-7037(87)90295-X).
- Schlaikjer A, Thomsen K, Kontogeorgis GM. Simultaneous description of activity coefficients and solubility with eCPA. *Ind Eng Chem Res*. 2017;56:1074–89. <https://doi.org/10.1021/acs.iecr.6b03333>.
- Young TF, Machin JS. Heat content and heat capacity of aqueous sodium chloride solutions. *J Am Chem Soc*. 1936;58:2254–60. <https://doi.org/10.1021/ja01302a049>.
- Cohen-Adad R, Vallée P, Lorimer JW. Sodium chloride. In: Cohen-Adad R, Lorimer JW, editors. Alkali metal and ammonium chlorides in water and heavy water (binary systems), vol. 47., Solubility data series Oxford: Pergamon Press; 1991. p. 64–209.
- Mal'tseva NN, Khain VS. Borogidrid natriya (sodium borohydride). Moscow: Nauka; 1985.
- Arkhangelskii IV, Tarasov VP, Kravchenko OV, Kirakosyan G, Tsvetkov MV, Solovov MV, Dobrovolskii YA, Shihovzev AV. Thermoanalytical and NMR investigation of NaBH<sub>4</sub>·2H<sub>2</sub>O thermolysis process. *J Therm Anal Calorim*. 2018;132:155–63. <https://doi.org/10.1007/s10973-017-6821-3>.
- Sharma A, Tyagi VV, Chen CR, Buddhi D. Review on thermal energy storage with phase change materials and applications. *Renew Sust Energy Rev*. 2009;13:318–45. <https://doi.org/10.1016/j.rser.2007.10.005>.
- Zeng JL, Shu L, Jiang LM, Chen YH, Zhang YX, Xie T, Sun LX, Cao Z. Thermodynamic and thermal energy storage properties of a new medium-temperature phase change material. *J Therm Anal Calorim*. 2019;135:3171–9. <https://doi.org/10.1007/s10973-018-7530-2>.
- Guo L, Yu X, Gao D, Guo Y, Ma C, Deng T. Synthesis and thermal energy storage properties of a calcium-based room temperature phase change material for energy storage. *J Therm Anal Calorim*. 2019;135:3215–21. <https://doi.org/10.1007/s10973-018-7610-3>.
- Xu X, Zhang X, Zhou S, Wang Y, Lu L. Experimental and application study of Na<sub>2</sub>SO<sub>4</sub>·10H<sub>2</sub>O with additives for cold storage. *J*

- Therm Anal Calorim. 2019;136:505–12. <https://doi.org/10.1007/s10973-018-7633-9>.
25. Lowitz TE. Observations on the crystallization of common salt under cooling and the new way of purification of the salt. *Nova Acta Acad Sci.* 1794;8:364–9 (**in Latin**).
26. Lowitz TE. Selected works on chemistry and chemical technology. Moscow: Publishing House of the USSR Academy of Sciences; 1955. p. 174–8 (**Russian translation**).

**Publisher's Note** Springer Nature remains neutral with regard to jurisdictional claims in published maps and institutional affiliations.